

Supporting Information

Vinylene-bridged naphthalenediimide-based dual-acceptor copolymers for thin-film transistors and solar steam generation

Chia-Yang Lin,^{†a} Guan-Lin Wu,^{†b} Ting-Yu Wang,^b Waner He,^a Ying-Sheng Wu,^b Shunsuke Imaoka,^a Shohei Shimizu,^a Wen-Chang Chen,^{b,c} Yoshimitsu Sagara,^a Chu-Chen Chueh,^{b,} and Tsuyoshi Michinobu^{a,*}*

Dr. C.-Y. Lin, Dr. W. He, S. Imaoka, S. Shimizu, Prof. Y. Sagara, and Prof. T. Michinobu

^a Department of Materials Science and Engineering, Institute of Science Tokyo, Tokyo 152-8552 Japan.

G.-L. Wu, T.-Y. Wang, Y.-S. Wu, Prof. W.-C. Chen, and Prof. C.-C. Chueh

^b Department of Chemical Engineering, National Taiwan University, Taipei 106, Taiwan.

Prof. W.-C. Chen

^c Advanced Research Center for Green Materials Science and Technology, National Taiwan University, Taipei 10617, Taiwan

*Corresponding authors E-mail: michinobu.t.aa@m.titech.ac.jp (T. M); cchueh@ntu.edu.tw (C.-C. C)

[†]These authors equally contributed to this work.

Keywords: Naphthalenediimide; vinylene bridge; dual-acceptor; thin-film transistors; solar steam generation

Experimental Section

Instruments. ^1H NMR spectra were recorded using a Bruker DPX400 MHz NMR spectrometer in CDCl_3 . Microwave polymerization was carried out using a Biotage microwave reactor in a 5 mL vessel sealed under a nitrogen atmosphere. The number-average molecular weight (M_n) values of the polymers were measured using gel permeation chromatography (GPC) at 40 °C. The chromatography was equipped with an Enshine SUPER CO-150, polystyrene gel columns (Stryagel HR 2 and stryagel 4), and eluent chloroform at a flow rate of 1.0 mL min^{-1} . Calibration was performed using standard polystyrene. Thermogravimetric analysis (TGA) was performed using a TA instrument Q50-TG thermogravimetry at a ramping rate of 10 °C min^{-1} . UV-visible-near infrared absorption spectra were recorded using a Hitachi U-4100 spectrophotometer. Steady-state fluorescence spectra of the films were monitored with an Ocean Optics QEProFL equipped with an LLS-385 LED light source and a Reflection/Backscattering Probe R400-7-UV-VIS; these spectra were not corrected. For film spectra, the polymer solution (3 mg mL^{-1}) was spin-coated onto a quartz substrate. Time-resolved fluorescence measurements were carried out with a Hamamatsu Photonics Quantaaurus-Tau. Quantum efficiencies were measured with a Hamamatsu Photonics Quantaaurus-QY. Cyclic voltammetry (CV) was measured using a CHI 627E electrochemical analyzer, which consists of a three-electrode cell system with ITO as the working electrode and platinum wire as the auxiliary electrode. Ag/AgCl and KCl (saturated) reference electrodes were used to determine the cell potential. The electrochemical properties of the polymer films were measured in anhydrous acetonitrile with 0.1 M tetrabutylammonium perchlorate as the electrolyte. All atomic force microscopy (AFM) images were obtained with a Bruker NanoWizard Sense with an OMCL-AC240TS cantilever under air at room temperature (r.t.). Surface mechanical properties were evaluated in the AFM contact mode. The films used for two-dimensional (2D) grazing incidence wide-angle X-ray scattering (GIWAXS) measurements were prepared on 1.5×1.5 cm^2 Si substrates. Measurements were conducted at the National Synchrotron Radiation Research Center (NSRRC) beamline 17A1 in Taiwan, with a wavelength of 1.32129 Å and an incident angle of 0.12 °.

Syntheses of the monomers.

Synthesis of vNDI. Precursor (500 mg, 0.42 mmol), (*E*)-1,2-bis(tributylstannyl)ethene (1.52 g, 2.52 mmol), and tetrakis(triphenylphosphine) palladium (9.7 mg, 0.0084 mmol) were added to toluene (125 mL) in a two-necked flask with a stir bar. The solution was degassed for 15 minutes and heated up to 90 °C

overnight. After cooling to room temperature, the solvent was removed under vacuum. The crude product was purified by silica gel column chromatography. A yellow oil was obtained (yield: 232 mg, 34.5 %). The ^1H NMR is presented in **Figure S1**.

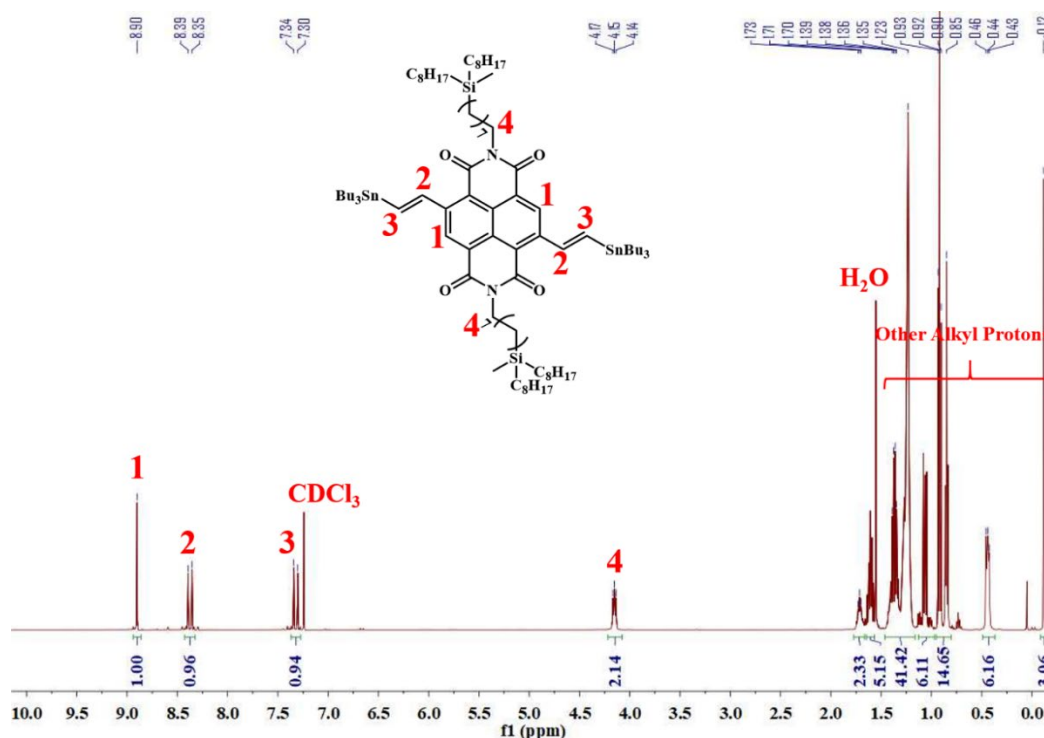


Figure S1. ^1H NMR of vNDI in CDCl_3 .

Synthesis of S / N / NS / NN. 4,7-Dibromo-5,6-difluoro-2,1,3- benzothiadiazole (334 mg, 1 mmol) / 4,7-dibromo-2-(2-ethylhexyl)-5,6-difluoro-2*H*-benzotriazole (425 mg, 1 mmol) / 4,8-dibromo-6-(2-ethylhexyl)-[1,2,5]thiadiazolo[3,4-*f*]benzotriazole (447 mg, 1 mmol) / 4,8-dibromo-2,6-bis(2-ethylhexyl)-2*H*-benzo[1,2-*d*:4,5-*d'*]bis([1,2,3]triazole)-6-ium-5-ide (542 mg, 1 mmol), tributyl(selenophen-2-yl)stannane (1050 mg, 2.5 mmol) and tetrakis(triphenylphosphine)palladium (34.7 mg, 0.03 mmol) were added to toluene in a two-neck flask with a stir bar. The solution was degassed for 15 minutes and heated up to 90 °C overnight. After cooling to room temperature, the solvent was removed under vacuum. The crude was purified by silica gel column chromatography. The orange / yellow solid and *N*-bromosuccinimide were

then added to CF in a single-neck flask. Acetic acid was added dropwise afterwards. The reaction was left in the dark and stirred overnight. The solvent was removed under vacuum, and the crude was purified by silica gel chromatography. The products **S** / **N** / **NS** / **NN** were obtained as red solid / light orange solid / light orange solid / light orange solid. Their ^1H NMR are presented in **Figure S2-S5**.

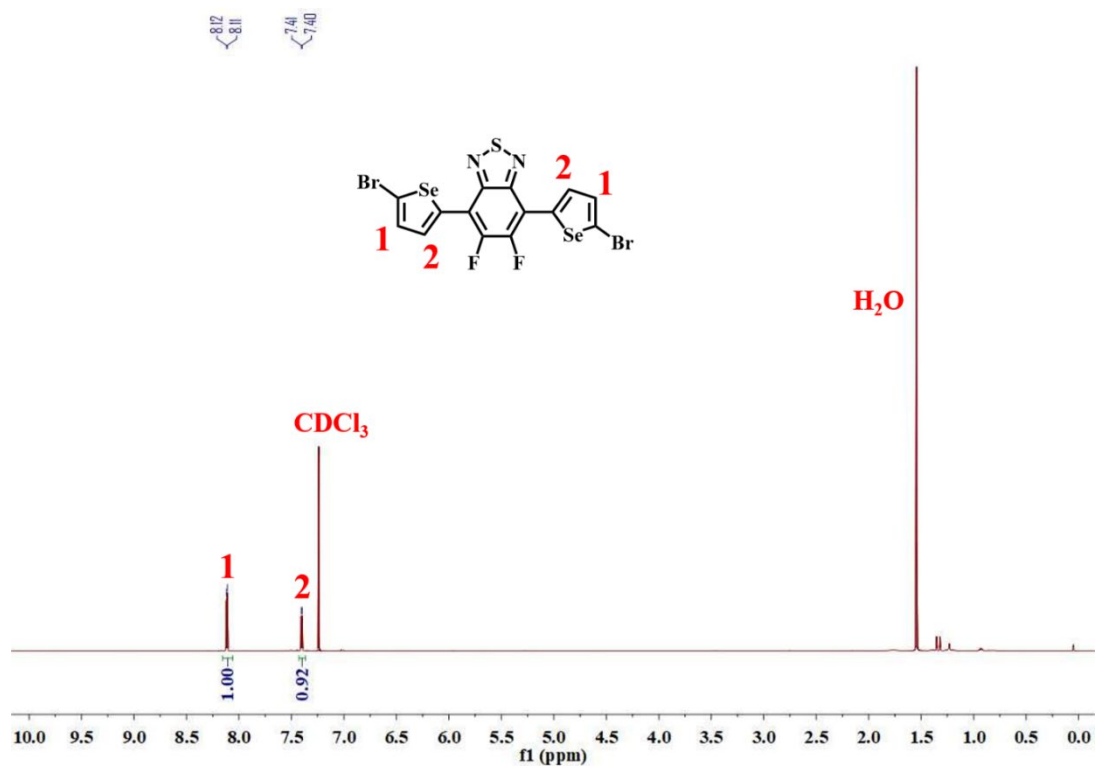


Figure S2. ^1H NMR of **S** in CDCl_3 .

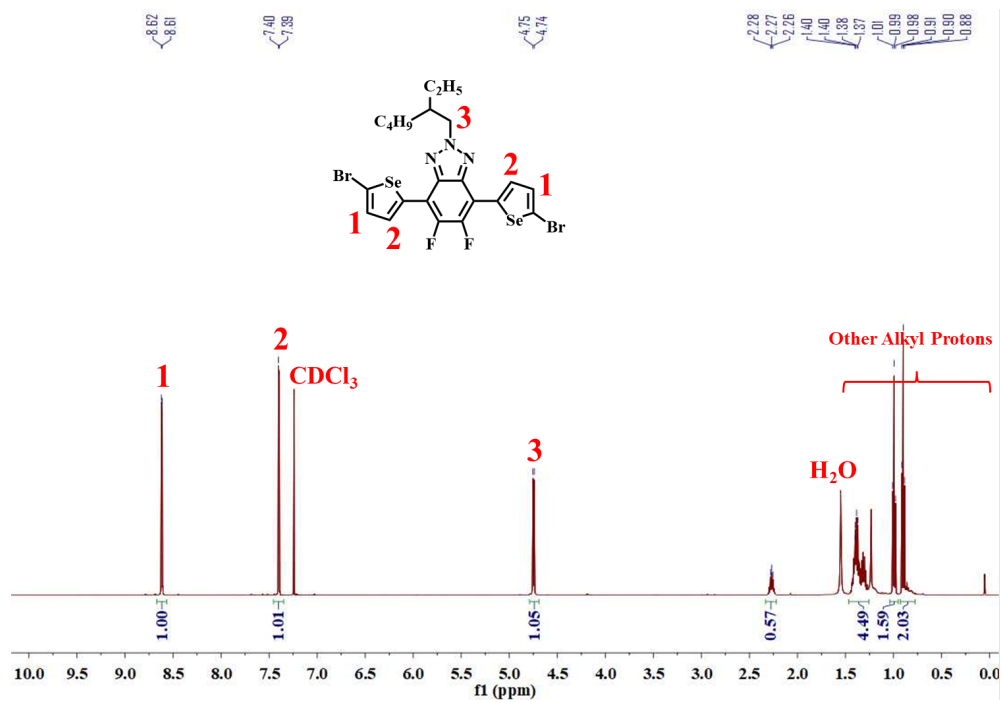


Figure S3. ^1H NMR of **N** in CDCl_3 .

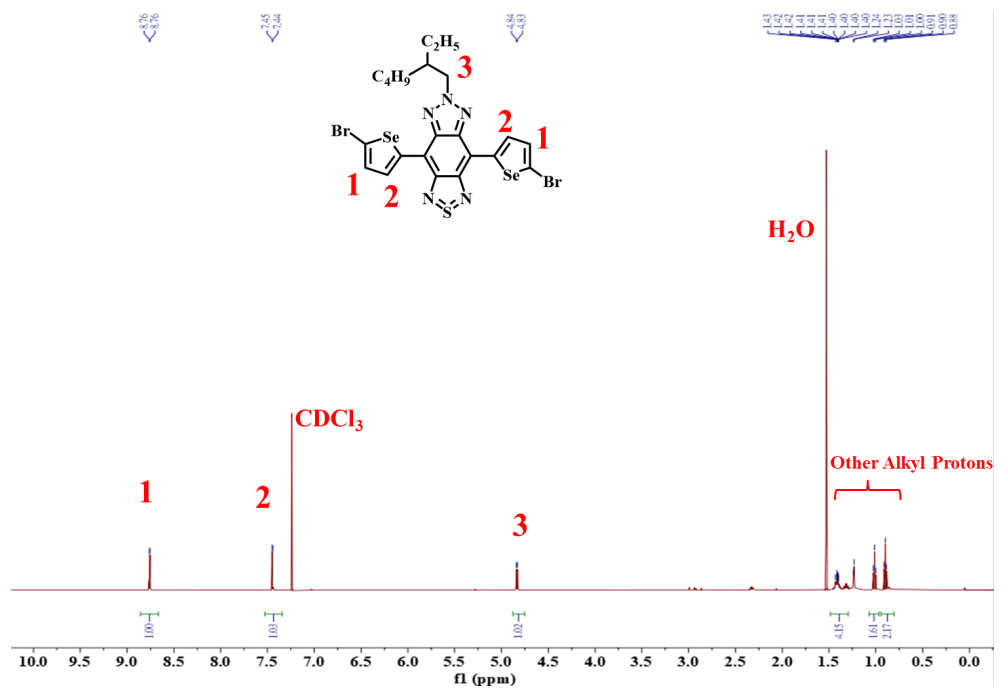


Figure S4. ^1H NMR of **NS** in CDCl_3 .

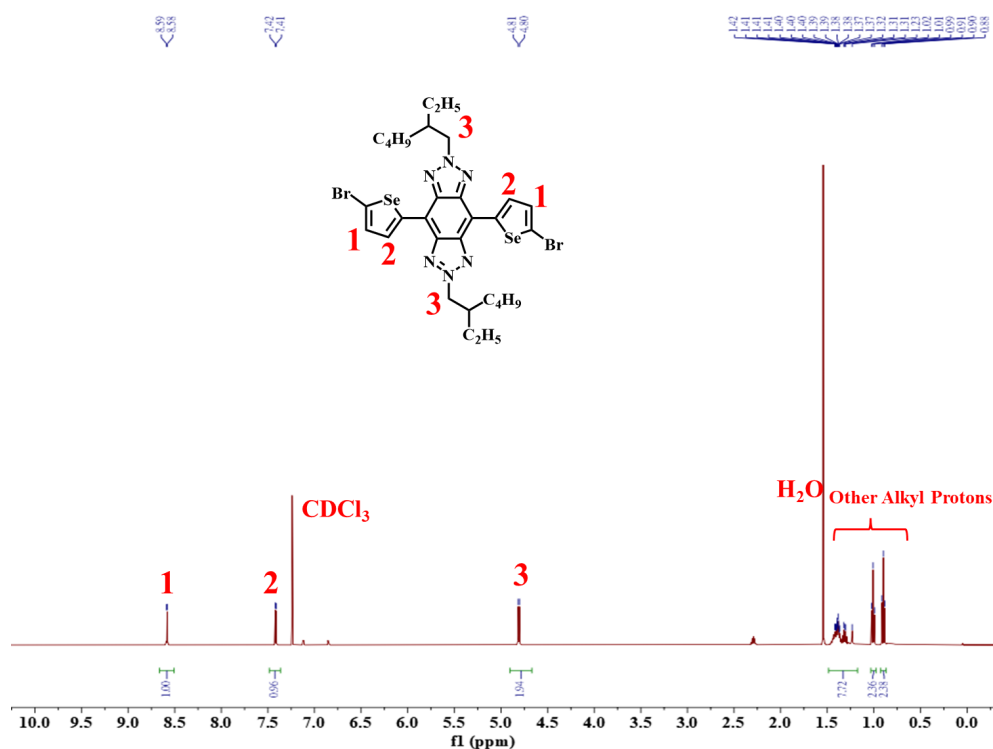


Figure S5. ^1H NMR of NN in CDCl_3 .

Detailed information of the target copolymers (vNDI-S/N/NS/NN).

vNDI-S. vNDI (116 mg, 0.071 mmol), S (41.7 mg, 0.071 mmol), $\text{Pd}(\text{PPh}_3)_4$ (4.1 mg, 0.0036 mmol), and chlorobenzene (3.0 mL). Dark solid (yield: 42.4 mg, 41.0 %). Anal. Calcd. For $[\text{C}_{82}\text{H}_{116}\text{F}_2\text{N}_4\text{O}_4\text{SSe}_2\text{Si}_2]$: C, 65.3; H, 7.9; N, 3.7; S, 2.1. Found: C, 63.2; H, 7.6; N, 3.8; S, 2.2. Molecular weight determined by GPC: $M_n = 33 \text{ kg mol}^{-1}$, $M_w/M_n = 2.7$. ^1H NMR is presented in **Figure S6**.

vNDI-N. vNDI (116 mg, 0.071 mmol), N (48.5 mg, 0.071 mmol), $\text{Pd}(\text{PPh}_3)_4$ (4.1 mg, 0.0036 mmol), and chlorobenzene (3.0 mL). Dark solid (yield: 49.0 mg, 44.5 %). Anal. Calcd. For $[\text{C}_{90}\text{H}_{133}\text{F}_2\text{N}_5\text{O}_4\text{Se}_2\text{Si}_2]$: C, 67.4; H, 8.5; N, 4.4. Found: C, 66.0; H, 9.2; N, 5.1. Molecular weight determined by GPC: $M_n = 47 \text{ kg mol}^{-1}$, $M_w/M_n = 2.3$. ^1H NMR is presented in **Figure S7**.

vNDI-NS. vNDI (116 mg, 0.071 mmol), NS (50.1 mg, 0.071 mmol), $\text{Pd}(\text{PPh}_3)_4$ (4.1 mg, 0.0036 mmol), and chlorobenzene (3.0 mL). Dark solid (yield: 39.6 mg, 37.9%).

Anal. Calcd. For $[C_{90}H_{133}N_7O_4SSe_2Si_2]$: C, 66.6; H, 8.2; N, 6.0; S, 2.0. Found: C, 64.8; H, 8.7; N, 6.2. Molecular weight determined by GPC: $M_n = 7 \text{ kg mol}^{-1}$, $M_w/M_n = 1.2$. 1H NMR is presented in **Figure S8**.

vNDI-NN. vNDI (116 mg, 0.071 mmol), NN (56.9 mg, 0.071 mmol), $Pd(PPh_3)_4$ (4.1 mg, 0.0036 mmol), and chlorobenzene (3.0 mL). Dark solid (yield: 49.0 mg, 44.5 %). Anal. Calcd. For $[C_{98}H_{150}N_8O_4Se_2Si_2]$: C, 68.4; H, 8.8; N, 6.5. Found: C, 66.5; H, 9.3; N, 6.8. Molecular weight determined by GPC: $M_n = 8 \text{ kg mol}^{-1}$, $M_w/M_n = 1.8$. 1H NMR is presented in **Figure S9**.

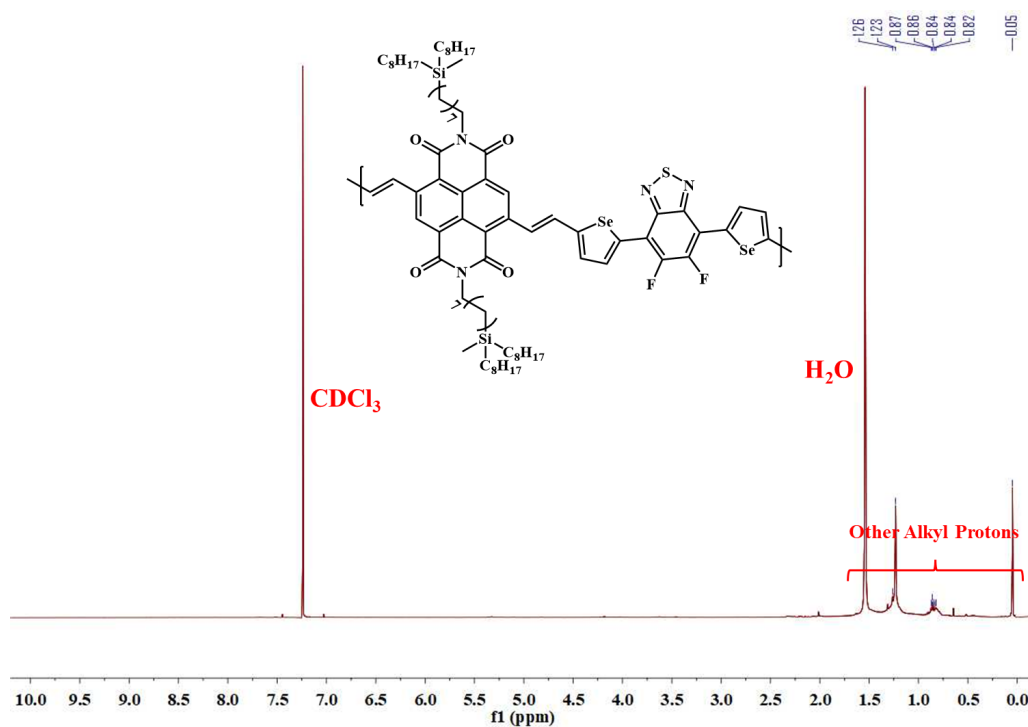


Figure S6. 1H NMR of vNDI-S in $CDCl_3$.

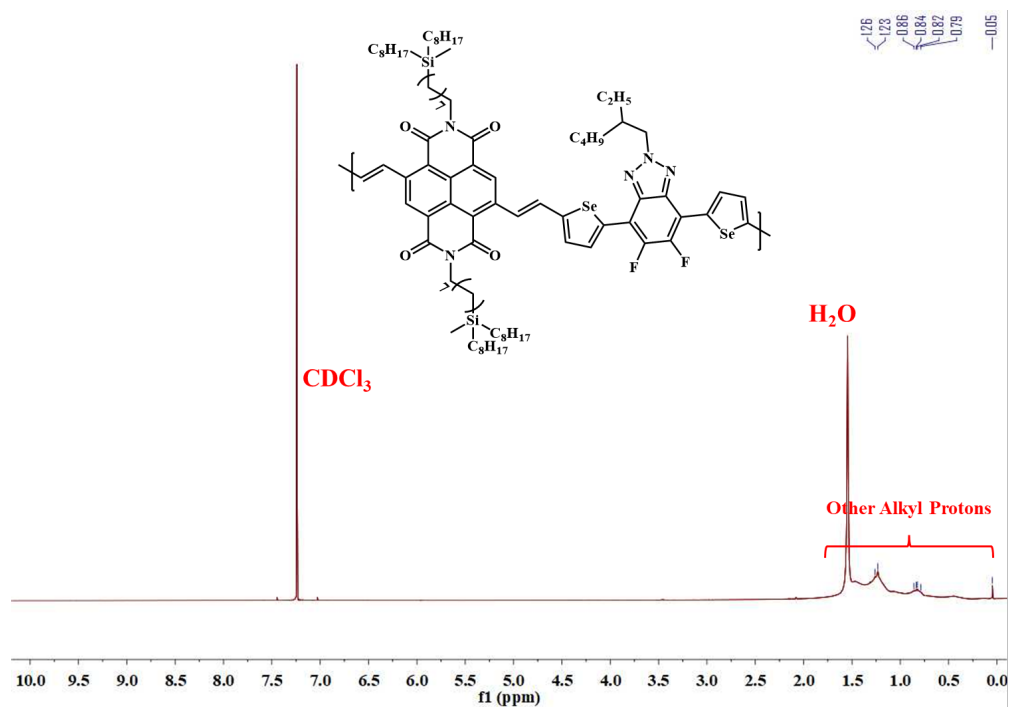


Figure S7. ¹H NMR of vNDI-N in CDCl₃.

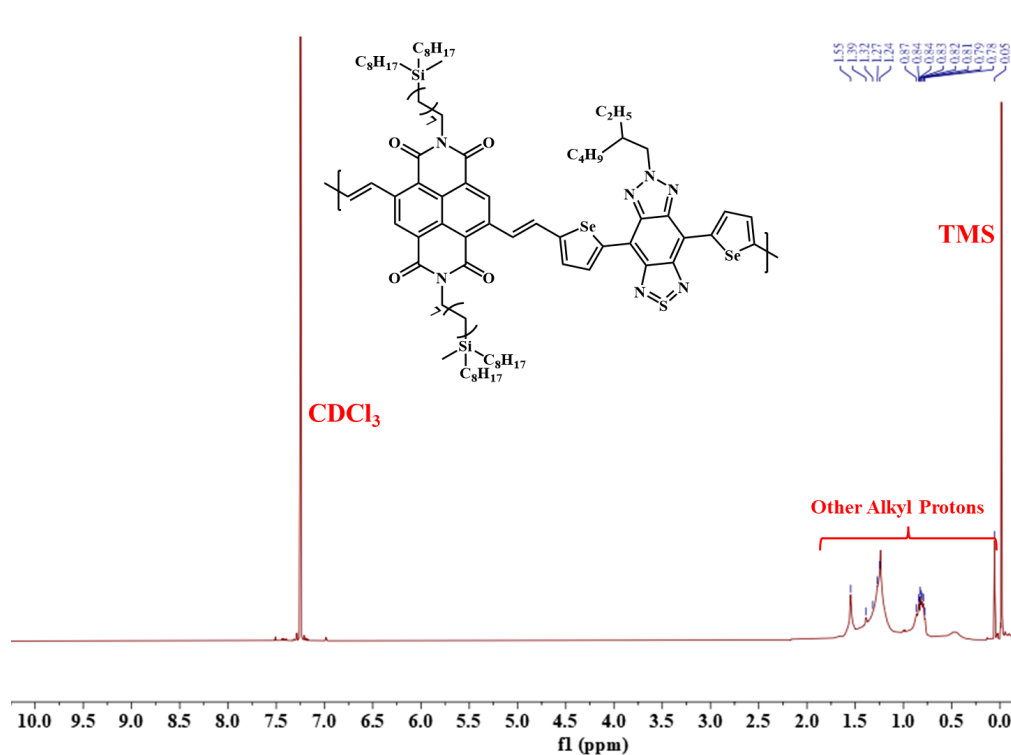


Figure S8. ¹H NMR of vNDI-NS in CDCl₃.

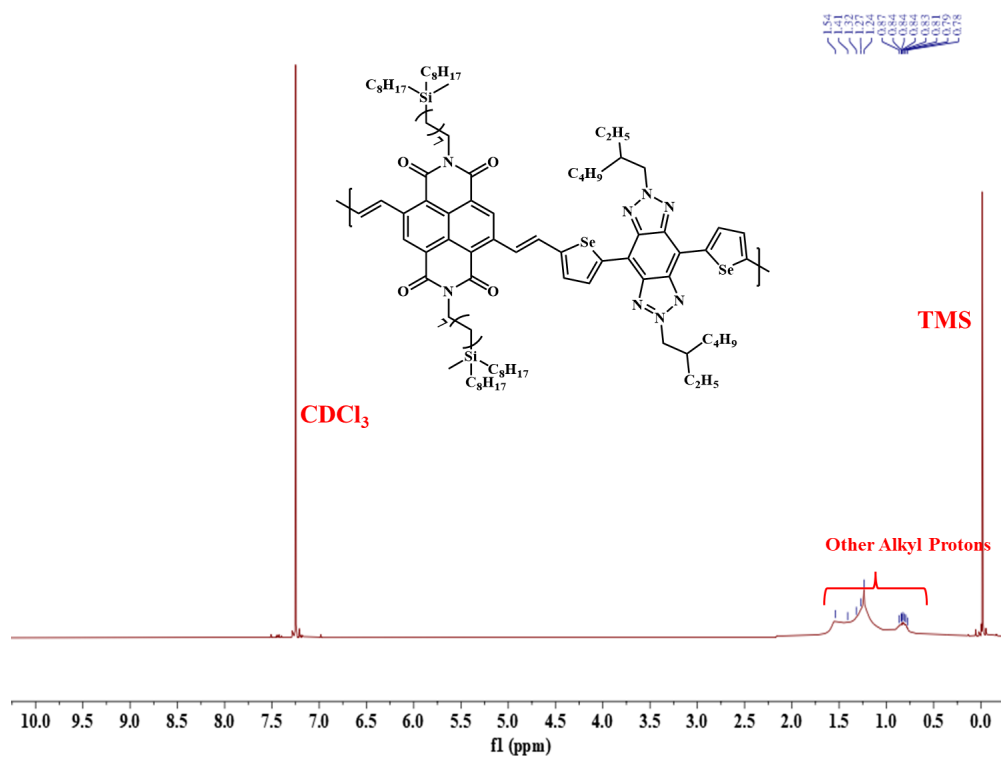


Figure S9. ^1H NMR of vNDI-NN in CDCl_3 .

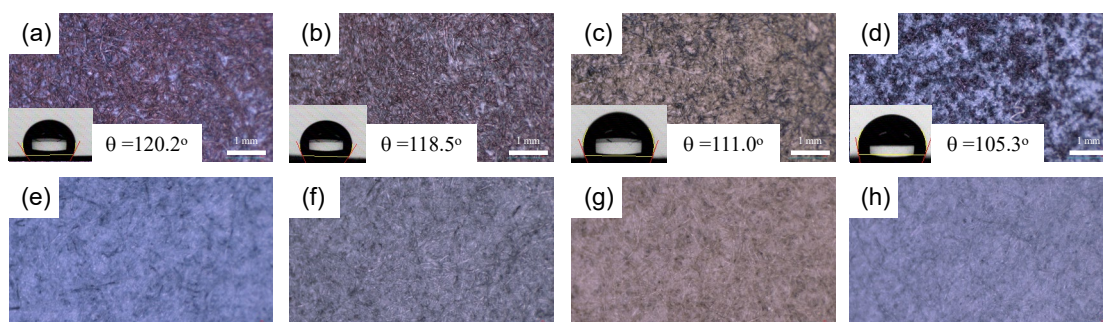


Figure S10. Surface morphology of the photothermal membranes observed under an optical microscope. (a-d) Top surfaces and (e-h) bottom surfaces of (a, e) vNDI-S, (b, f) vNDI-N, (c, g) vNDI-NS, and (d, h) vNDI-NN films, respectively. Insets: Water contact angle images of the top surfaces. The scale bar is 1 mm.

Table S1. PL properties of vNDI-based polymer films

	λ_{em} (nm) ^a	Φ_f ^b	τ (ns) ^c	k_r (10^9 s ⁻¹) ^d	k_{nr} (10^9 s ⁻¹) ^e
vNDI-S	904	0.01	1.48	0.007	0.67
vNDI-N	900	0.008	1.86	0.004	0.53

^a Peak emission wavelength. ^b Fluorescence quantum yield. ^c Fluorescence lifetime.

^d Radiative decay rate constant. ^e Non-radiative decay rate constant.

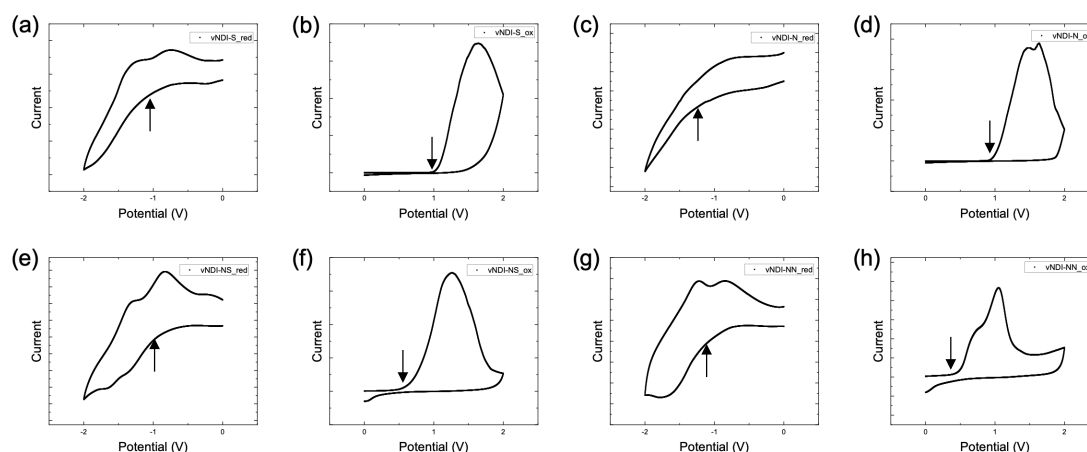


Figure S11. CV curves measured in acetonitrile with 0.1 M tetrabutylammonium perchlorate for polymer films. (a, c, e, g) Reduction and (b, d, f, h) oxidation curves for vNDI-S, vNDI-N, vNDI-NS, and vNDI-NN, respectively.

Table S2. Energy levels of vNDI-based polymers

	E_{HOMO} (eV) ^a	E_{LUMO} (eV) ^a	E_{g} (eV) ^a	$E_{\text{HOMO_calc}}$ (eV) ^b	$E_{\text{LUMO_calc}}$ (eV) ^b	$E_{\text{g_calc}}$ (eV) ^b
vNDI-S	-5.78	-3.64	2.14	-5.31	-3.56	1.75
vNDI-N	-5.73	-3.55	2.18	-5.18	-3.44	1.74
vNDI-NS	-5.46	-3.80	1.66	-4.90	-3.72	1.18
vNDI-NN	-5.23	-3.68	1.55	-4.80	-3.49	1.31

^a Estimated from cyclic voltammetry. ^b Values calculated by DFT.

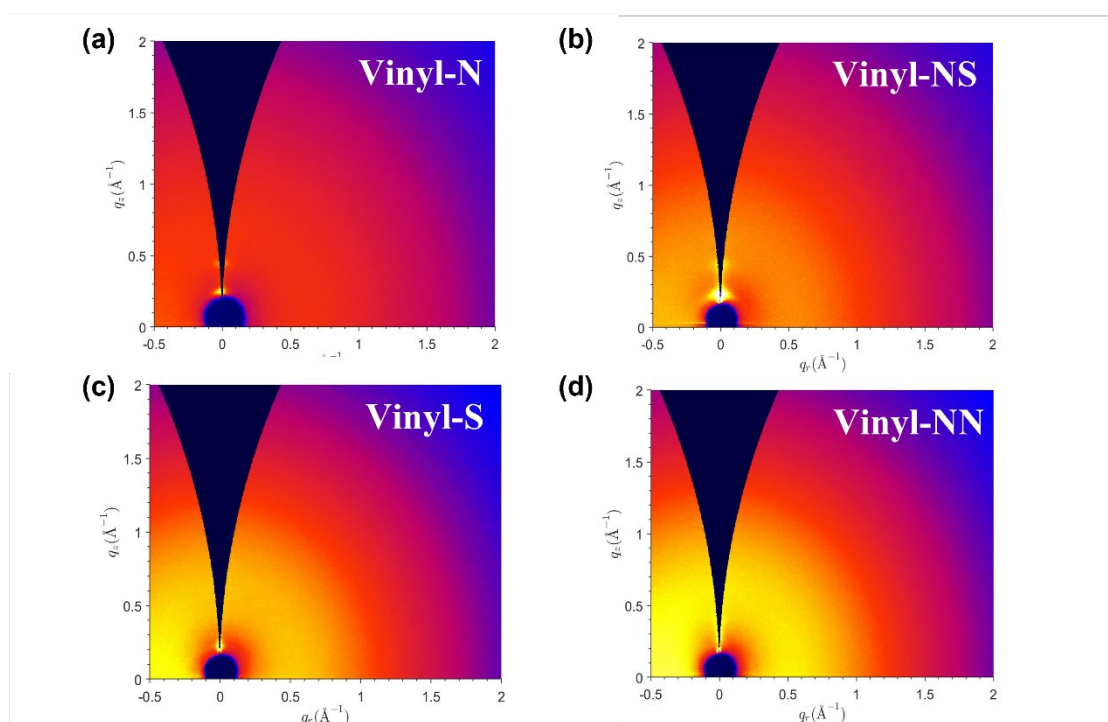


Figure S12. 2D GIWAXS patterns of vNDI-based polymer films.

Table S3. Summary of crystalline coherent length (CCL) and *d*-spacing (DS) of vNDI-based polymer films.

	100		200		300	
	CCL (Å)	DS (Å)	CCL (Å)	DS (Å)	CCL (Å)	DS (Å)
vNDI-S	33.36	26.33	18.23	14.01	-	-
vNDI-N	165.15	23.95	98.98	13.95	27.04	9.88
vNDI-NS	97.58	26.78	75.72	14.20	26.97	10.10
vNDI-NN	39.66	24.19	104.28	14.53	-	-

Table S4. Summary of transistor characteristics of the OFET devices based on vNDI-based polymer films under optimized thermal annealing conditions.

	<i>T</i> (°C)	μ_e (cm ² V ⁻¹ s ⁻¹)	I_{on} / I_{off}	V_{th} (V)	μ_h (cm ² V ⁻¹ s ⁻¹)	I_{on} / I_{off}	V_{th} (V)
vNDI-S	200	7.95 x 10 ⁻³ (1.01 x 10 ⁻²)	10 ⁵ ~10 ⁶	46.7	1.34 x 10 ⁻³ (2.01 x 10 ⁻³)	10 ⁴	-69.3
vNDI-N	250	1.10 x 10 ⁻² (1.22 x 10 ⁻²)	10 ⁵ ~10 ⁶	54.5	1.02 x 10 ⁻² (1.28 x 10 ⁻²)	10 ⁵ ~10 ⁶	-23.9
vNDI-NS	250	3.13 x 10 ⁻³ (4.30 x 10 ⁻³)	10 ² ~10 ⁴	57.3	6.12 x 10 ⁻⁴ (7.46 x 10 ⁻³)	10 ³ ~10 ⁴	-34.3
vNDI-NN	250	1.38 x 10 ⁻⁴ (2.49 x 10 ⁻⁴)	10 ³ ~10 ⁴	52.6	2.08 x 10 ⁻⁴ (2.57 x 10 ⁻⁴)	10 ³	-25.0